Enhancement effect of carbon adsorbent on ozonation of aqueous phenol

Jintawat Chaichanawong, Takuji Yamamoto*, Takao Ohmori

Research Institute for Innovation in Sustainable Chemistry, National Institute of Advanced Industrial Science and Technology (AIST), 1-1-1 Higashi, Tsukuba, Ibaraki 305-8565, Japan

ABSTRACT

Removal of aqueous phenol was examined by the simultaneous use of ozone and porous carbon adsorbents possessing different porous structures and surface properties. The removal efficiency of aqueous phenol was higher with the simultaneous use of ozone and carbon adsorbents than the use of ozone alone, due to the adsorptive-concentration effect of the adsorbents. The enhancement effect of macroporous carbon cryogel beads (CCB) on the ozonation of aqueous phenol was confirmed to be greater than in microporous activated carbon beads. Introduction of acidic functional groups to CCB by liquid-phase oxidation significantly diminished the adsorptive-concentration effect of CCB, since the interaction of aqueous phenol with the surface of CCB decreased.

© 2009 Elsevier B.V. All rights reserved.

1. Introduction

The pollution of water by organic compounds remains a serious problem, since wastewater is often released from industrial factories without any effective treatment. Phenolic compounds, which are highly toxic substances that damage human health and aquatic life, are common contaminants in wastewater. They are widely used in industrial processes for synthesizing pharmaceutical and petrochemical products. Conventional treatment methods, such as biodegradation, adsorption by activated carbon, and chemical oxidation have been proposed for purifying wastewater which contains phenolic compounds [1–4]. However, the removal of phenolic compounds by conventional methods is usually inefficient. The development of an efficient wastewater treatment process is therefore needed. Advanced oxidation processes (AOPs) have been widely investigated, since they are a promising method for the degradation of organic compounds [5–8]. AOPs are oxidation processes that generate reactive oxidizing agents such as hydroxyl radicals, which are more reactive than molecular O_3 or H_2O_2, and are highly effective in degrading organic compounds in wastewater because of their rapid and nonselective reaction with nearby electron-rich organic compounds [9]. The major advantage of AOPs is that they have the potential to completely remove organic pollutants. The contaminants can be readily degraded to stable inorganic compounds such as water, carbon dioxide and salts. In most AOPs, oxidation agents such as ozone (O_3) and H_2O_2, ultraviolet (UV) irradiation, are used alongside catalysts to efficiently generate hydroxyl radicals. The simultaneous use of ozone with porous materials such as titanium dioxide, activated carbon, zeolite, or silica gel, can enhance the degradation of phenolic compounds in wastewater [10–12].

For wastewater which contains phenolic compounds, various types of microporous activated carbon have been commonly employed as adsorbents or supporting materials of catalysts because of their large surface area [13–15]. However, the small diffusivity of molecules in micropores (IUPAC definitions: $d_p < 2$ nm; d_p denotes pore diameter) of activated carbon in a liquid phase appears to limit both removal efficiency and its regeneration [13]. Porous carbon possessing many mesopores or macropores in addition to micropores is considered to be more suitable than conventional activated carbon as adsorbents or support materials for catalysts. Some activated carbons (e.g., bamboo or charcoal) are known to possess mesopores and/or macropores [16,17], and are expected to be applicable to the above purposes. However, researchers have been faced with the technical challenge of controlling their morphology so as to create beads or fibers that are suitable for use in water treatment processes. To the best of our knowledge, no activated carbon with many macropores and the desired morphology has yet been developed.

A carbon gel, which possesses a controlled morphology and many mesopores with a moderate number of micropores, is regarded as a potential adsorbent for use in AOPs because of the ease of mass transfer. Formation of macropores in addition to mesopores and micropores is considered to be favorable for increasing the performance of the adsorbents in AOPs. One method of developing macropores in a carbon gel is to adjust the initial pH of the

---

solution of carbon precursors to the acidic range. Moreno-Castilla et al. [18] synthesized carbon gels with many macropores featuring micropores by using acetates of transition metals as catalysts for the sol–gel polycondensation of resorcinol with formaldehyde. The porous structure of the carbon gels strongly depended on the species of metal acetate, which affects the initial pH of the solution and consequently the sol–gel chemistry. The carbon gels which were prepared using acetates of nickel or cobalt as the catalyst possessed both macropores and micropores, whereas the carbon gels prepared using iron or copper acetate possessed only macropores.

The surface properties of adsorbents also significantly affect their performances. There have been several findings on the surface modification of activated carbons or carbon gels [19–22]. However, the effect of surface modification on their performance as adsorbents for AOPs has not been studied sufficiently.

Hence, in the present study, carbon cryogel beads (CCB) which are a kind of carbon gel, are synthesized as a model material, and their performance as an adsorbent in AOPs employing ozone is examined. The enhancement effect of CCB on the ozonation of aqueous phenol is then examined by comparing the performance of CCB with that of conventional activated carbon beads. The influence of surface modification by liquid-phase oxidation on the performance of the adsorbent is further investigated.

2. Experimental

2.1. Preparation of CCB

A resorcinol–formaldehyde (RF) aqueous solution was prepared in the following manner. Distilled water after ion-exchange treatment was used as a solvent. The ratios of resorcinol to formaldehyde (R/F) and resorcinol to water (R/W) were fixed at 0.5 mol/mol and 0.25 g/cm^3, respectively. Under the conditions, carbon cryogels show developed mesoporosity by employing sodium carbonate as a catalyst for the sol–gel polycondensation [23,24]. In this study, to obtain macroporous carbon, Ni acetate was used as a catalyst. The Ni content in the reactants (R + F) was fixed at 1.0 wt.% [25]. All chemicals were purchased from Wako Pure Chemical Industries, Inc. (Osaka, Japan) as research grade chemicals. The prepared RF solutions were first kept at 298 K for 1 h before starting injection to effect the sol–gel polycondensation. The RF hydrogel beads were synthesized from the prepared solutions based on the SI method [23,25]. In the SI method, the RF solutions are injected via a syringe pump into silicone oil which is circulated in a Teflon tube. Monodisperse droplets of the RF solution were formed as a result. The droplets were collected in an oil bath kept at 363 K and quickly gelled to produce monodisperse RF hydrogel beads. The obtained hydrogel beads were washed with cyclohexane and ethanol, respectively, and then immersed in t-butanol for 24 h (3 times). The hydrogel beads were then freeze-dried at 263 K for 24 h under vacuum to obtain carbon precursor beads, and subsequently carbonized at 1273 K for 4 h in an inert atmosphere to obtain CCB.

The surface of the CCB was oxidized by immersing the beads in 1.0 mol/l (NH$_4$)$_2$S$_2$O$_8$ solution for different periods of time. The surface-modified CCB oxidized for 24 h were labeled as CCB$_{ox}$ and their performance was compared with virgin CCB.

Microporous activated carbon beads (G-70R), whose average particle diameter is about 0.8 mm, were supplied from Kureha Corp. and also used as an adsorbent after heating in an air flow at 463 K.

2.2. Characterization of carbon adsorbents

The number of acidic functional groups attached to the surface of the CCB and G-70R was measured by NH$_3$-TPD (temperature-programmed desorption). The porous structure of CCB was
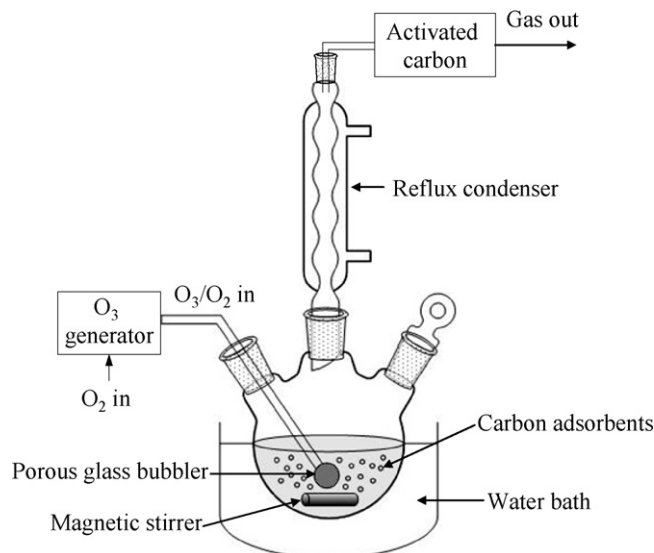

Fig. 1. A batch reactor used for degradation of aqueous phenol.

observed using a scanning electron microscope (S-3400N SEM, Hitachi Ltd., Japan) and a scanning transmission electron microscope (HD-2000 STEM, Hitachi Ltd., Japan). The porous properties of the carbon adsorbents were determined using the nitrogen gas adsorption method. Adsorption and desorption isotherms of nitrogen were measured at 77 K using an automatic adsorption and desorption apparatus (BEL mini, BEL Japan Inc., Japan). All samples were outgassed at 383 K in a vacuum for 12 h prior to measurement. The Brunauer–Emmett–Teller surface areas (S_{BET}) of the samples were evaluated based on the adsorption isotherms. Pore size distribution of the sample was determined by applying the DFT method. Mesopore volume (V_{mes}) and micropore volume (V_{mic}) were estimated by applying the α_s-plot to the adsorption isotherms. The apparent density (ρ_{app}) was estimated from the weight and volume of the beads. The skeletal density (ρ_s) was measured using a helium pycnometer (Accupyc 1330, Micromeritics Instrument Corp., GA, USA), and the total pore volume (V_t) was calculated based on the following relationship.

$$V_t = \frac{1}{\rho_{app}} - \frac{1}{\rho_s} \qquad (1)$$

The macropore volume was then estimated from the equation below.

$$V_{mac} = V_t - V_{mes} - V_{mic} \qquad (2)$$

2.3. Liquid-phase adsorption of phenol using carbon adsorbents

20 mg of CCB, CCB$_{ox}$ and G-70R were added to 40 ml of phenol aqueous solutions at different initial concentrations (12.5–400 ppm), and the mixtures were shaken in a water bath at 303 K for 4 days. The equilibrium concentration of phenol was then measured using a UV–vis spectrophotometer (UV-2450, Shimadzu Corporation) at a wavelength of 270 nm. The spent carbon adsorbents after the liquid-phase adsorption of phenol were regenerated by washing in ethanol at 298 K for 21 h.

2.4. Ozonation of aqueous phenol in the presence of carbon adsorbents

Fig. 1 shows the batch reactor used for the degradation of aqueous phenol by simultaneous use of ozone with the carbon adsorbents. The experimental conditions are summarized in

Table 1
Experimental condition for degradation of aqueous phenol.

Parameter	Condition
Initial concentration of phenol (C_0) [mg/l]	200, 400
Volume of phenol solution [cm^3]	200
Reaction temperature [K]	303
Flow rate of O_3/O_2 into a reactor [cm^3/min]	500
Weight of carbon adsorbent [g]	0.5

Table 1. Ozone-containing oxygen gas was introduced to the solution using a porous glass bubbler which was placed at the bottom of the reactor. The average ozone concentration in aqueous solution was adjusted to 10 mg/l. The mixture was agitated using a magnetic stirrer at a stirring rate of 200 rpm. The transient changes in phenol concentration were then measured using a high performance liquid chromatograph (HPLC, LC-10A, Shimadzu Corporation) equipped with a UV detector. Total organic carbon (TOC) concentration was measured by a TOC analyzer (Sievers 900, GE Analytical Instruments Inc.). To study the effect of adsorption of phenol on the ozonation, the transient change of aqueous phenol by adsorption on the carbon adsorbent was measured using the same experimental apparatus without supplying ozone.

3. Results and discussion

3.1. Porous properties of carbon adsorbents

Fig. 2(a) shows optical microscope images of CCB: they possess a perfectly spherical shape with a mean diameter of about 1 mm. As shown in Fig. 2(b) and (c), CCB consist of interconnected primary nanoparticles. The size of the particles ranges from several tens to hundreds of nanometers. The interconnection of the primary particles results in the formation of a unique network with many mesopores and macropores present between the nanoparticles.

Fig. 3 shows adsorption and desorption isotherms of nitrogen on carbon adsorbents at 77 K, and the corresponding pore size distributions obtained by analysis of the isotherms. According to the IUPAC definitions, the isotherms of nitrogen on CCB and CCB$_{ox}$ are
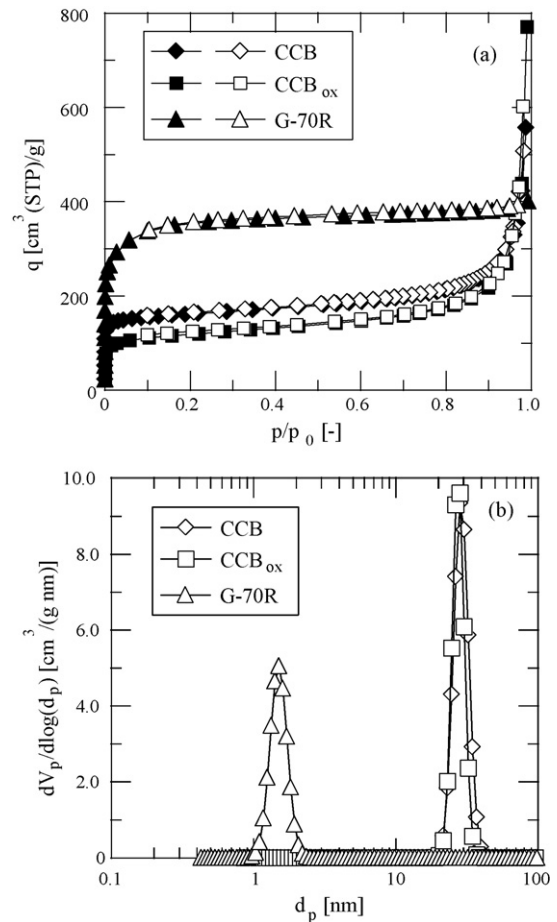

Fig. 3. (a) Adsorption and desorption isotherms of nitrogen on carbon adsorbents at 77 K (closed symbols: adsorption; open symbols: desorption), and (b) corresponding pore size distributions.
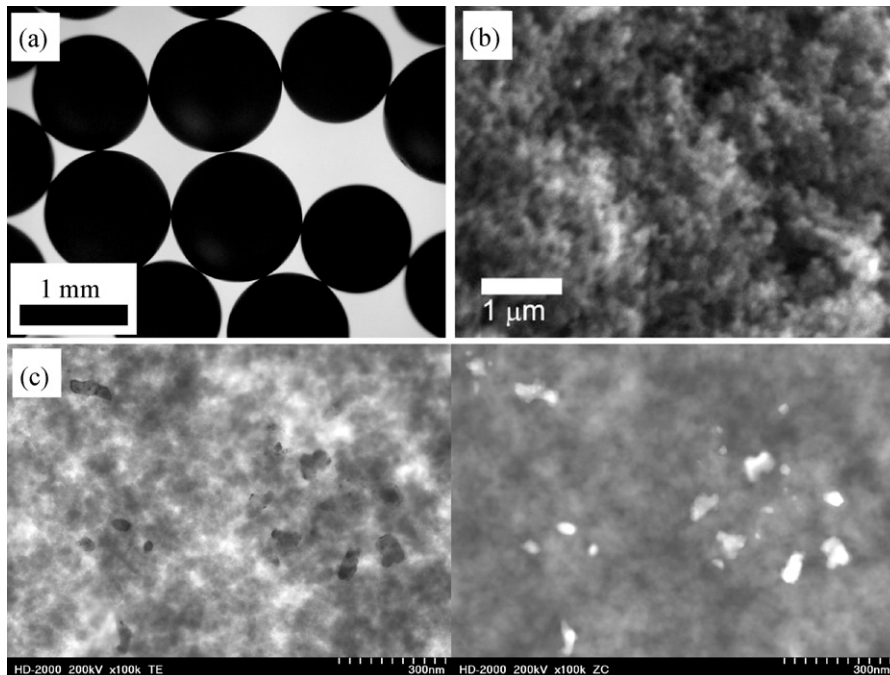

Fig. 2. (a) CCB, (b) SEM image of porous structure, (c) STEM images of primary nanoparticles: bright field image (left) and dark field image (right).

Table 2
Properties of the carbon adsorbents.

Sample	Number of regeneration	S_{BET} [m²/g]	V_{mic} [cm³/g]	V_{mes} [cm³/g]	V_{mac} [cm³/g]	d_{peak}[a] [nm]	AFG[b] [×10⁻⁶ mol/(g m²)]
CCB	Original	598	0.18	0.27	3.22	28.3	1.24
	1	179	0.01	0.18	3.48	21.6	NM[c]
	2	156	0.01	0.17	3.49	20.2	NM
	3	145	ND[d]	0.18	3.49	20.2	NM
CCB$_{ox}$	Original	422	0.11	0.31	3.45	28.3	13.10
	1	420	0.11	0.29	3.49	24.7	NM
	2	382	0.10	0.31	3.46	23.1	NM
	3	321	0.07	0.12	3.68	24.7	NM
G-70R	Original	1281	0.51	0.05	ND	1.5	0.24
	1	979	0.38	0.05	ND	1.5	NM
	2	835	0.33	0.04	ND	1.5	NM
	3	775	0.30	0.04	ND	1.5	NM

[a] The peak pore diameter of the pore size distribution.
[b] Density of acidic functional groups. AFG is calculated by dividing the adsorbed amount of NH₃ with the BET specific surface area.
[c] Not measured.
[d] Not detected.

classified into Type II, which are observed with macroporous materials allowing for unrestricted monolayer–multilayer adsorption to occur at a relatively high pressure range ($p/p_0 \approx 1$) [26]. In the SEM image (Fig. 2(b)) and the STEM images (Fig. 2(c)), it can be seen that CCB possess large amount of macropores. In contrast, the isotherm of nitrogen on G-70R is classified into Type I, showing a very small external surface area and the enhanced adsorbent–adsorbate interactions in micropores of molecular dimensions. It is clear that both CCB and CCB$_{ox}$ possess a broad pore size distribution that ranges from large mesopores to macropores as expected, whereas the G-70R shows a fairly sharp pore size distribution in the range of micropores. The porous properties of the carbon adsorbents are summarized in Table 2. The BET surface area and the volume of micropores of CCB are smaller than those of G-70R. Interestingly, the BET surface area and the volume of micropores of CCB decrease as a result of surface modification, whereas mesopores and the number of acidic functional groups significantly increase, probably because the micropores are partially enlarged by the introduction of the acidic functional groups.

3.2. Adsorption characteristics of carbon adsorbents

Fig. 4 shows the effect of immersion time of carbon adsorbents in $(NH_4)_2S_2O_8$ solution on the number of acidic functional groups introduced. The number of acidic functional groups significantly increases at the early 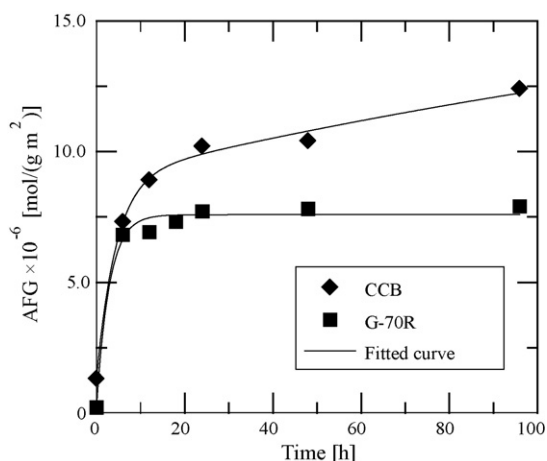stage of the liquid-phase oxidation and slightly increases with the increase in immersion time after 24 h. The amount of acidic functional groups on the carbon adsorbents per unit BET surface area (S_{BET}) were estimated and are summarized in Table 2. Since the amount of acidic functional groups on CCB$_{ox}$ is significantly larger than those on virgin CCB and G-70R, the introduction of acidic functional groups to the carbon surface by the liquid-phase oxidation can be confirmed.

Fig. 5 shows the liquid-phase adsorption characteristics of the carbon adsorbents. All adsorption isotherms of phenol can be fitted by the Freundlich equation, which involves multilayer sorption of heterogeneous surfaces, i.e.:

$$q = K_F C^{1/n} \tag{3}$$

where q and C denote the equilibrium adsorption capacity and concentration of adsorbate in the solution at equilibrium. K_F and $1/n$ are Freundlich parameters, which are related to the adsorption capacity and the heterogeneity of the adsorption sites, respectively [27,28].

The Freundlich parameters are summarized in Table 3. The amount of phenol adsorbed on G-70R, which shows the largest S_{BET}, was larger than those on CCB and CCB$_{ox}$. The difference in the amount of adsorbed phenol on CCB and G-70R can be attributed to the difference in specific surface areas. However, it should be noted that the amount of adsorbed phenol on CCB$_{ox}$ is almost half as much as that on CCB, although the S_{BET} of CCB$_{ox}$ is about 80% of that of CCB. The predominant reason for this is the decreased
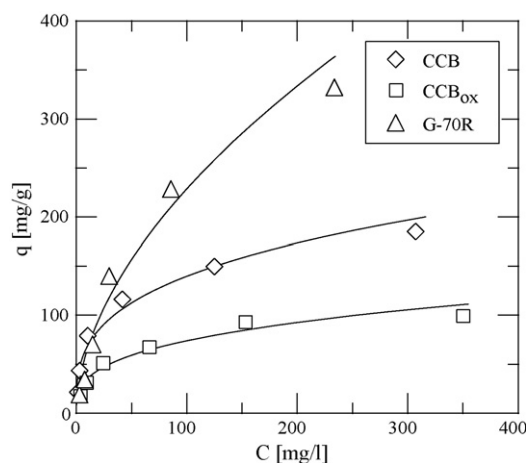

Fig. 4. Relation between oxidation time and amount of acidic functional groups introduced to CCB and G-70R. [$(NH_4)_2S_2O_8$] = 1 mol/l, oxidation temperature = 298 K.

Fig. 5. Liquid-phase adsorption isotherm of phenol on carbon adsorbents at 303 K, solid line: Freundlich plot.

Table 3
Freundlich parameters.

Sample	Times of repetitive adsorption	Freundlich parameter		r^2 [–]
		$1/n$ [–]	K_F [mg/g]	
CCB	1st	0.31	33.3	0.97
	2nd	0.21	26.8	0.97
	3rd	0.24	13.6	0.88
	4th	0.21	12.7	0.68
CCB$_{ox}$	1st	0.32	16.7	0.95
	2nd	0.39	11.9	0.99
	3rd	0.45	8.9	0.96
	4th	0.28	13.3	0.99
G-70R	1st	0.55	18.5	0.95

r^2: correlation coefficient in the fitting by the Freundlich equation.

interaction of aqueous phenol with the surface of CCB$_{ox}$. It was previously reported that functional groups such as carboxyl (–COOH), ketone (–CO–), lactone (–CO–O–), ether (–O–) and phenolic (–OH) groups could be introduced to the carbon surface by the liquid-phase oxidation using the same chemical as that we used in this study [29]. These acidic functional groups are believed to increase the polarity of the carbon surface, resulting in the enhancement of water adsorption in preference to phenol. The adsorption of water molecules is thus considered to interfere with phenol molecules accessing the adsorption sites [13,30–32]. Thus, the adsorption capacity of carbon adsorbents strongly depends not only on the porous structure but also on the surface properties.

To further study the surface property of CCB, the effect of repetitive regeneration of CCB and CCB$_{ox}$ on liquid-phase adsorption isotherms of aqueous phenol was examined, as shown in Fig. 6. It is noteworthy that the adsorption capacity of CCB after regeneration significantly decreases, whereas that of CCB$_{ox}$ hardly changes, even after repeating regeneration three times. This is because the irreversible adsorption of phenol on CCB$_{ox}$ can be prevented by the introduction of acidic functional groups to the surface of CCB [20]. As summarized in Table 2, the significant decrease in the micropore volume of CCB is attributed to the irreversible adsorption of phenol or reaction products on the micropores. Based on these results, it can be concluded that the regeneration efficiency can be increased by the surface modification of CCB. Although the acidic functional groups can prevent the irreversible adsorption of phenol, they also limit the accessibility of phenol molecules to the adsorption sites [30–32].

3.3. Ozonation of aqueous phenol in the presence of carbon adsorbents

To investigate the adsorptive-concentration effect of carbon adsorbents on ozonation, removal of aqueous phenol was first examined using carbon adsorbents alone and ozone alone, respectively. The ozonation of aqueous phenol in the presence of carbon adsorbents was then examined using the same reactor. Fig. 7 shows the transient changes in concentration of aqueous phenol and the reaction rate during the treatment. The closed symbols and open symbols respectively correspond to the changes in the concentra-

Table 4
Rate constant of phenol degradation.

Carbon adsorbents	k [min^{-1}]	r^2 [–]
Only ozone	0.094	0.98
CCB	0.253	0.99
CCB$_{ox}$	0.106	0.98
G-70R	0.224	0.99

k: removal rate constant of phenol by ozonation.
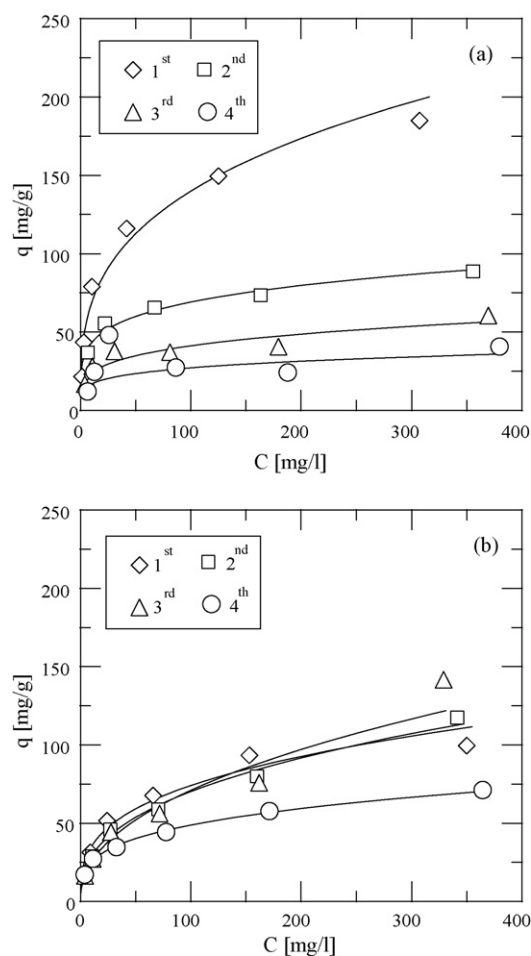r^2: correlation coefficient.

Fig. 6. Effect of repetitive regeneration on liquid-phase adsorption isotherms of phenol on (a) CCB and (b) CCB$_{ox}$ at 303 K, solid line: Freundlich plot.

tion of phenol when using carbon adsorbents alone and the case of simultaneous use of ozone with carbon adsorbents. As shown in Fig. 7, the adsorptive-concentration of aqueous phenol on carbon adsorbents is correlated to their liquid-phase adsorption characteristics. In the case of simultaneous use of CCB with ozone, the removal efficiency is greater than the case of using CCB$_{ox}$.

The removal rate constant is determined by fitting the measured data to the following Eq. (4),

$$-\frac{dC_{ph}}{dt} = kC_{ph} \tag{4}$$

where C_{ph}, t, and k respectively denote the concentration of phenol, treatment time and removal rate constant of ozonation. Here, we assume that the reaction order of the ozonation is equal to one.

As summarized in Table 4, the removal rate constant of ozonation when using only ozone is estimated to be 0.094 min^{-1}. In the case of simultaneous use of CCB with ozone, the removal rate constant of ozonation can be increased to 0.253 min^{-1}, whereas in the case of simultaneous use of CCB$_{ox}$ with ozone, the rate constant was 0.106 min^{-1}, and it was almost the same as that when using only ozone. This is because the adsorptive-concentration of phenol hardly occurred on CCB$_{ox}$, as can be assumed from the results shown in the previous section. In the case of simultaneous use of G-70R with ozone, the rate constant is 0.224 min^{-1}. When CCB or G-70R is used during ozonation, the rate constant is approximately twice as large as that when using ozone alone. This indicates that degradation of phenol can be enhanced by the adsorptive-concentration effect of CCB or G-70R. It is also confirmed that
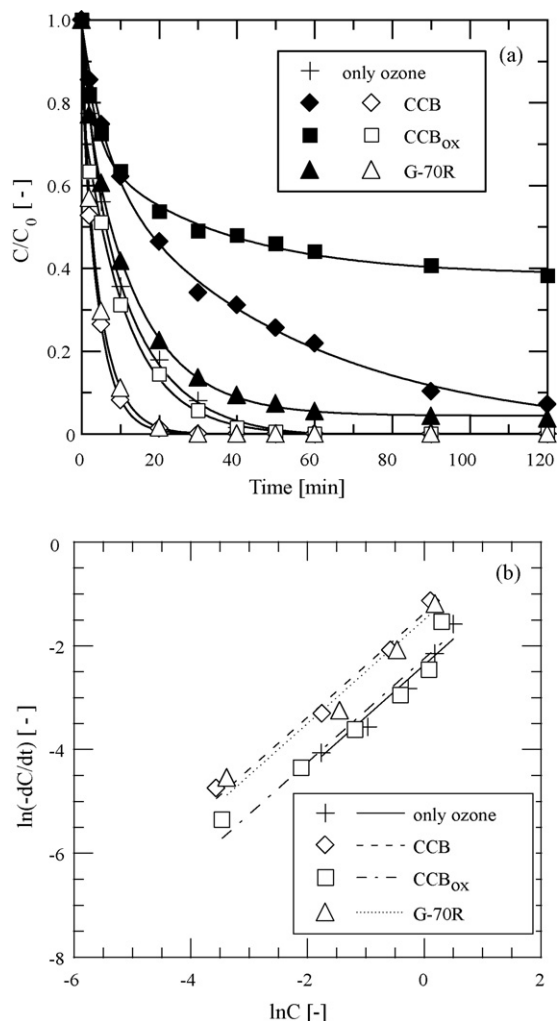
Fig. 7. Transient changes in concentration of aqueous phenol during ozonation at 303 K; closed symbols: carbon adsorbent only, open symbols: carbon adsorbent + ozone. $C_0 = 200$ mg/l.

the adsorption rate of phenol can be related to the average pore size of the carbon adsorbent. By applying the Dünwald–Wagner equation [33] to the results shown in Fig. 7, the intra-particle diffusion coefficient of phenol in CCB, CCB$_{ox}$ and G-70R was estimated as 8.11×10^{-11}, 7.70×10^{-11} and 5.93×10^{-11} m^2/s, respectively. Since diffusion of phenol or reaction products in CCB, which possess many macropores, is likely to be easier than in G-70R, it consequently leads to an increase in removal efficiency. Here, it should be noted that the catalytic effect of the nickel oxide contained in CCB is negligible, since the particle size is quite large (60 nm < average diameter < 100 nm) and the particles are almost entirely encapsulated by the matrix of the carbon gel.

The transient changes in TOC concentrations during the ozonation are shown in Fig. 8. In the case of the ozonation in the presence of CCB or G-70R, the TOC concentration could be reduced to less than 25 ppm by the treatment for 120 min. On the other hand, in the case of the simultaneous use of CCB$_{ox}$ with ozone, the TOC concentration at the treatment time of 120 min was about 100 ppm, which was almost the same as the result of using only ozone. The order of enhancement of the carbon adsorbent on ozonation is CCB > G-70R > CCB$_{ox}$, and is the same as that of the degradation of phenol as summarized in Table 4. It has been reported that the intermediate products such as benzoquinone, catechol, hydroquinone, etc. could be generated during the degradation of phenol by advanced oxidation process [6]. In the case of ozonation in the presence of CCB or
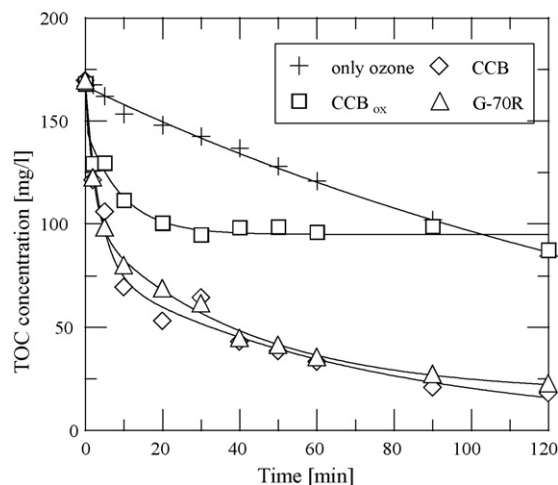

Fig. 8. Transient changes in TOC concentration during ozonation of aqueous phenol at 303 K. $C_0 = 200$ mg/l.

G-70R, the intermediate products could be effectively removed by adsorption on CCB or G-70R. In contrast, the intermediate products hardly adsorbed on CCB$_{ox}$. Consequently, the final concentration of TOC in the case of using CCB$_{ox}$ with ozone is almost the same as that in the case of using only ozone. Based on the results, we conclude that degradation of phenol or TOC can be enhanced by the adsorptive-concentration effect of CCB or G-70R.

Fig. 9 shows the effect of surface modification and repetitive regeneration of CCB on ozonation of aqueous phenol. The removal efficiency of phenol gradually decreases with an increase in the number of times of regeneration when CCB are used. This is probably due to the irreversible adsorption of phenol or reaction products formed by degradation of phenol on micropores of CCB. On the other hand, when using CCB$_{ox}$, the removal efficiency of phenol was lower than that when using CCB. However, the decrease in removal efficiency is significantly smaller. This result confirms that surface modification of CCB is effective in preventing irreversible adsorption of phenol or reaction products. However, the acidic functional groups attached to the surface of CCB interfere with the adsorption of phenol molecules to the adsorption sites. To improve the removal efficiency of phenol, further study is needed to determine the optimum conditions for surface modification of CCB.
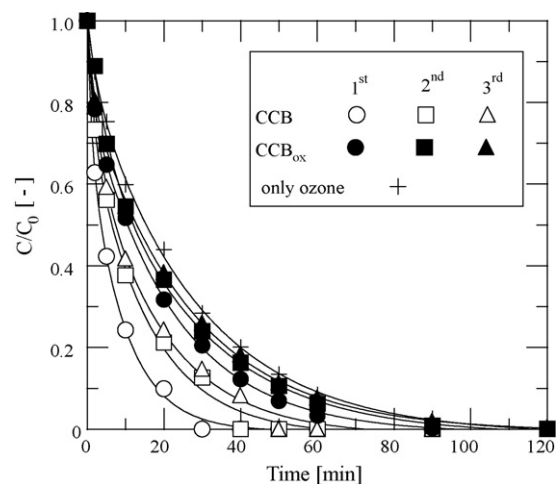

Fig. 9. Effect of surface modification on degradation of aqueous phenol during ozonation at 303 K and its regeneration. $C_0 = 400$ mg/l.

4. Conclusions

Ozonation of aqueous phenol was examined by the simultaneous use of ozone and carbon adsorbents with different porous structures and surface properties. The removal efficiency of phenol by the simultaneous use of ozone with carbon adsorbents was higher than that when using ozone alone, confirming the clear adsorptive-concentration effect of the adsorbents. CCB showed a higher enhancement effect than G-70R due to the presence of macropores. The surface of the CCB was modified by liquid-phase oxidation using $(NH_4)_2S_2O_8$ solution. The regeneration efficiency of phenol could be increased by surface modification of CCB, whereas the amount of phenol adsorbed on CCBs decreased as a result of surface modification. Although the removal efficiency of phenol by simultaneous use of ozone and surface-modified CCB (CCB_{ox}) changed little after repetitive regeneration, the removal efficiency was lower than when using CCB as adsorbents.

The authors believe that a high-performance water treatment process can be developed by simultaneous use of macroporous carbon adsorbents with ozone. The enhancement effect that results from using porous adsorbents on water treatment has potential for use in other AOP systems employing UV or ultrasound, and will be examined in future studies.

Acknowledgements

References

[1] R.L. Autenrieth, J.S. Bonner, Akgerman, M. Okaygun, E.M. McCreary, Biodegradation of phenolic wastes, J. Hazard. Mater. 28 (1991) 29–53.
[2] W. Tanthapanichakoon, P. Ariyadejwanich, P. Japthong, K. Nakagawa, S.R. Mukai, H. Tamon, Adsorption–desorption characteristics of phenol and reactive dyes from aqueous solution on mesoporous activated carbon prepared from waste tires, Water Res. 39 (2005) 1347–1353.
[3] R.S. Juang, T.P. Chung, M.L. Wang, D.J. Lee, Experimental observations on the effect of added dispersing agent on phenol biodegradation in a microporous membrane bioreactor, J. Hazard. Mater. 151 (2008) 746–752.
[4] G. Busca, S. Berardinelli, C. Resini, L. Arrighi, Technologies for the removal of phenol from fluid streams: a short review of recent developments, J. Hazard. Mater. 160 (2008) 265–288.
[5] B. Gözmen, B. Kayan, A.M. Gizir, A. Hesenov, Oxidative degradations of reactive blue 4 dye by different advanced oxidation methods, J. Hazard. Mater. 168 (2009) 129–136.
[6] M. Pimentel, N. Oturan, M. Dezotti, M.A. Oturan, Phenol degradation by advanced electrochemical oxidation process electro-Fenton using a carbon felt cathode, Appl. Catal. B: Environ. 83 (2008) 140–149.
[7] E.J. Rosenfeldt, K.G. Linden, S. Canonica, U. von Gunten, Comparison of the efficiency of OH radical formation during ozonation and the advanced oxidation processes O_3/H_2O_2 and UV/H_2O_2, Water Res. 40 (2006) 3695–3704.
[8] J. Qu, Research progress of novel adsorption processes in water purification: a review, J. Environ. Sci. 20 (2008) 1–13.
[9] J.C. Crittenden, R.R. Trusssell, D.W. Hand, K.J. Howe, G. Tchobanoglous, Water Treatment Principle and Design, 2nd ed., John Wiley & Sons, 2005, pp. 582–586.
[10] S.H. Lin, C.H. Wang, Ozonation of phenolic wastewater in a gas-induced reactor with a fixed granular activated carbon bed, Ind. Eng. Chem. Res. 42 (2007) 1648–1653.
[11] N. Sano, T. Yamamoto, D. Yamamoto, S.I. Kim, A. Eiad-ua, H. Shinomiya, M. Nakaiwa, Degradation of aqueous phenol by simultaneous use of ozone with silica-gel and zeolite, Chem. Eng. Process. 46 (2007) 513–519.
[12] L. Lei, L. Gu, X. Zhang, Y. Su, Catalytic oxidation of highly concentrated real industrial wastewater by integrated ozone and activated carbon, Appl. Catal. A: Gen. 327 (2007) 287–294.
[13] Md. Ahmaruzzaman, Adsorption of phenolic compounds on low-cost adsorbents: a review, Adv. Colloid Interface Sci. 143 (2008) 48–67.
[14] L. Bo, X. Quan, Xi. Wang, S. Chen, Preparation and characteristics of carbon-supported platinum catalyst and its application in the removal of phenolic pollutants in aqueous solution by microwave-assisted catalytic oxidation, J. Hazard. Mater. 157 (2008) 179–186.
[15] G.L. Puma, A. Bono, D. Krishnaiah, J.G. Collin, Preparation of titanium dioxide photocatalyst loaded onto activated carbon support using chemical vapor deposition: a review paper, J. Hazard. Mater. 157 (2008) 209–219.
[16] W.M.A.W. Daud, W.S.W. Ali, Comparison on pore development of activated carbon produced from palm shell and coconut shell, Bioresour. Technol. 93 (2004) 63–69.
[17] D. Zhao, J. Zhang, E. Duan, J. Wang, Adsorption equilibrium and kinetics of dibenzothiophene from n-octane on bamboo charcoal, Appl. Surf. Sci. 254 (2008) 3242–3247.
[18] C. Moreno-Castilla, F.J. Maldonado-Hódar, A.F. Pérez-Cadenas, Physicochemical surface properties of Fe, Co, Ni, and Cu-doped monolithic organic aerogels, Langmuir 19 (2003) 5650–5655.
[19] H Tamon, M. Okazaki, Desorption characteristic of aromatic compounds in aqueous solution on solid adsorbents, J. Colloid Interface Sci. 179 (1996) 181–187.
[20] H. Tamon, M. Okazaki, Influence of surface oxides on ethanol regeneration of spent carbonaceous adsorbents, J. Colloid Interface Sci. 196 (1997) 120–122.
[21] A.P. Terzyk, Further insight into the role of carbon surface functionalities in the mechanism of phenol adsorption, J. Colloid Interface Sci. 268 (2003) 301–329.
[22] D. Borah, S. Satokawa, S. Kato, T. Kojima, Characterization of chemically modified carbon black for sorption application, Appl. Surf. Sci. 254 (2008) 3049–3056.
[23] T. Yamamoto, A. Endo, A. Eiad-ua, T. Ohmori, M. Nakaiwa, A. Soottitantawat, Synthesis of monodisperse carbon beads with developed mesoporosity, AIChE J. 53 (2007) 746–749.
[24] T. Yamamoto, T. Ohmori, Y.H. Kim, Preparation of monodisperse carbon cryogel microspheres, Micropor. Mesopor. Mater. 112 (2008) 211–218.
[25] J. Chaichanawong, T. Yamamoto, S.I. Kim, T. Ohmori, Preparation and characterization of nickel-modified carbon cryogel beads with uniform particle size, J. Non-Cryst. Solids 355 (2009) 1605–1612.
[26] F. Rouqerol, J. Rouquerol, K. Sing, Adsorption by Powders and Porous Solids, Academic Press, 1999, pp. 19–20.
[27] L. John Kennedy, J. Judith Vijaya, K. Kayalvizhi, G. Sekaran, Adsorption of phenol from aqueous solutions using mesoporous carbon prepared by two-stage process, Chem. Eng. J. 132 (2007) 279–287.
[28] V. Fierro, V. Torné-Fernández, D. Montané, A. Celzard, Adsorption of phenol onto activated carbons having different textural and surface properties, Micropor. Mesopor. Mater. 111 (2008) 276–284.
[29] C. Moreno-Castilla, F. Carrasco-Marín, A. Mueden, The creation of acid carbon surfaces by treatment with $(NH_4)_2S_2O_8$, Carbon 35 (1997) 1619–1626.
[30] A.P. Terzyk, The impact of carbon surface chemical composition on the adsorption of phenol determined at the real oxic and anoxic conditions, Appl. Surf. Sci. 253 (2007) 5752–5755.
[31] P.M. Álvarez, J.F. García-Araya, F.J. Beltrán, J.F. Masa, F. Medina, Ozonation of activated carbons: effect on the adsorption of selected phenolic compounds from aqueous solutions, J. Colloid Interface Sci. 283 (2005) 503–512.
[32] T. Asakawa, K. Ogino, Adsorption of phenol surface-modified carbon black from its aqueous solution, J. Colloid Interface Sci. 102 (1984) 348–355.
[33] H. Dünwald, C. Wagner, Methotik der Messung von Diffusionsgeschwindigkeiten bei Losungsvorgangen von Gasen in festen Phasen, Z. Phys. Chem. B24 (1934) 53–58.